Rossby Wave Ray Tracing in a Barotropic Divergent Atmosphere

CHUNGU LU*

NOAA/Earth System Research Laboratory, Boulder, Colorado

JOHN P. BOYD

Department of Atmospheric, Oceanic, and Space Science, University of Michigan, Ann Arbor, Michigan

(Manuscript received 12 June 2007, in final form 14 August 2007)

ABSTRACT

The effects of divergence on low-frequency Rossby wave propagation are examined by using the two-dimensional Wentzel–Kramers–Brillouin (WKB) method and ray tracing in the framework of a linear barotropic dynamic system. The WKB analysis shows that the divergent wind decreases Rossby wave frequency (for wave propagation northward in the Northern Hemisphere). Ray tracing shows that the divergent wind increases the zonal group velocity and thus accelerates the zonal propagation of Rossby waves. It also appears that divergence tends to feed energy into relatively high wavenumber waves, so that these waves can propagate farther downstream. The present theory also provides an estimate of a phase angle between the vorticity and divergence centers. In a fully developed Rossby wave, vorticity and divergence display a $\pi/2$ phase difference, which is consistent with the observed upper-level structure of a mature extratropical cyclone. It is shown that these theoretical results compare well with observations.

1. Introduction

Waves are one of the most prevalent phenomena in the atmosphere. During the propagation of atmospheric waves, the transport of the wave momentum and heat has a dramatic impact on the evolution of atmospheric circulation. Three atmospheric phenomena including the quasi-biennial oscillation (QBO) in the tropical stratosphere, stratospheric sudden warming (SSW) in the polar region, and the significant strengthening and speeding up of the upper-level jet stream have been successfully explained by wave propagation mechanisms. Lindzen and Holton (1968) studied the QBO in the tropical stratosphere using the theory of upward-propagating gravity waves and wave breaking. Matsuno (1971) explained the SSW as the interaction between an upward-propagating planetary wave and the mean flow at the wave's critical layer. Gao et al. (1990) explained the significant strengthening and speeding up of the upper-level jet stream using the generalized Eliassen–Palm (E–P) flux theory.

The aforementioned scientific findings are mainly supported by the propagation theories associated with gravity waves, planetary waves, and transient waves. It is well known that low-frequency waves have an important impact on weather and climate. There have been numerous observational and analysis studies on low-frequency phenomena. Wallace and Gutzler (1981) analyzed teleconnections using geopotential height data and verified existence of the North Pacific Oscillation (NPO) and the North Atlantic Oscillation (NAO). Madden and Julian (1971, 1972) found a low-frequency oscillation (LFO) with a 45–50-day period by analyzing wind and surface pressure fields in the tropics with a spectral method. Many studies showed that the LFO not only propagated along the equator but also possessed a northward component. Wallace and Blackmon (1983) discussed the causes of the LFO and showed that the low-frequency variation is similar to a two-dimensional Rossby wave train. Kiladis and Weickmann (1992, 1997) investigated the Rossby wave response (on various time scales) to tropical convection using outgoing longwave radiation (OLR) and National

* Also in collaboration with Colorado State University.

Corresponding author address: Dr. Chungu Lu, NOAA/Earth System Research Lab, Global System Division, Boulder, CO 80305.
E-mail: chungu.lu@noaa.gov

DOI: 10.1175/2007JAS2537.1

Centers for Environmental Prediction's (NCEP's) global analyses.

As shown in many previous works, the properties of 2D Rossby wave propagation can be studied by employing the nondivergent barotropic vorticity equation, linearized about a basic flow. Early studies were focused on differences between various basic flows. Bennett and Young (1971) considered a basic flow of constant latitudinal shear. Boyd (1978, 1982) investigated the effects of latitudinal shears on equatorial and global Rossby waves, respectively. Hoskins and Karoly (1981) developed a theory for Rossby wave propagation in a slowly varying zonally symmetric basic flow. Branstator (1983), Karoly (1983), and Hoskins and Ambrizzi (1993) examined Rossby wave propagation with zonally asymmetric basic flows. In particular, Branstator (1983) used a basic state that varies both in latitude and longitude, while Hoskins and Ambrizzi (1993) considered a basic state of a climatological 300-hPa December–February (DJF) time-mean flow. Some closed-form solutions were obtained from these studies using the Wentzel–Kramers–Brillouin (WKB) method, and these provide most of our present understanding of 2D Rossby wave propagation. The results from these classic studies will be reviewed in section 3.

It has long been recognized, ever since Rossby (1939), that the nondivergent vorticity equation does not properly take into account the adjustment of pressure and wind fields. Rossby (1945) and Yeh (1949) derived a Rossby wave dispersion relation that included divergence effects. This well-known result is included in many standard dynamics textbooks, for example, Kundu (1990). Cressman (1958) also investigated the effect of divergence on long atmospheric waves from a numerical weather prediction point of view. The most detailed study of the impact of tropical divergence on Rossby wave propagation was conducted by Sardeshmukh and Hoskins (1988). They concluded that the advection of vorticity by the divergent component of the horizontal flow is a significant term in the large-scale vorticity balance, and should not be ignored when investigating the effect of tropical heating on the circulation in middle latitudes. This study used a numerical approach to integrate the divergent barotropic vorticity equation because a closed-form solution was lacking. Though important insight was gained from the study, it did not investigate the Rossby wave ray-tracing problem.

Recently renewed interest in the interaction of tropics and extratropics has rekindled curiosity about Rossby wave propagation, as indicated by this new wave of investigations, particularly in the context of tropical western Pacific disturbances and high-impact weather systems across the Pacific basin (e.g., Ferranti et al. 1990; Chang and Yu 1999; Chang 2005; Hoskins and Hodges 2002; Klein et al. 2002; Hakim 2003; Parsons et al. 2006). One of the issues related to the connection of the North American weather system and Rossby wave packet propagation is the accurate prediction of the wave propagation path and the life cycle of tropical and extratropical storms. Despite the aforementioned studies, Rossby wave ray tracing for tropical and extratropical transitions (ET) is still missing. No doubt divergence will play an important role in the development and propagation of tropical disturbances into extratropical regions. The classic Rossby wave ray-tracing studies by Hoskins and Karoly (1981), Branstator (1983), Karoly (1983), and Hoskins and Ambrizzi (1993) have provided crucial insight into the Rossby wave propagation problem. However, their studies can be extended further by including divergence effects.

The propagation of the low-frequency wave has an important impact on the anomaly of the atmospheric circulation, which motivates us to further study this phenomenon. In this work, the effect of divergence on the development of the low-frequency Rossby waves is studied by analyzing the divergent barotropic vorticity equation. In section 2, we first conduct some observational analyses. These observations show possible Rossby wave trains with quite different paths and life cycles. We then conduct a review of some Rossby wave propagation theories and results from previous studies (section 3). In section 4, we consider the effect of divergence in the barotropic vorticity equation, and solve it by means of the WKB method. The effects of divergence on the WKB solutions are discussed. In section 5, we apply ray-tracing diagnostics to NCEP–National Center for Atmospheric Research (NCAR) reanalysis data and compare the results with observations. Our conclusions are given in section 6.

2. Observations of tropical and extratropical disturbance propagation in the Pacific Ocean basin

Because the tropical western Pacific Ocean is a large pool of warm water, it is a favorable location for the generation of atmospheric disturbances. Some of these disturbances develop into tropical cyclones, travel northwestward (steered by the tropical easterlies), and make landfall on many Southeast Asian countries (during typhoon season, typically from August to October). These storms often cause major casualties and property damage in that part of the world. Another group of these disturbances form various wave packets, which travel northeastward (quickly caught by the midlatitude

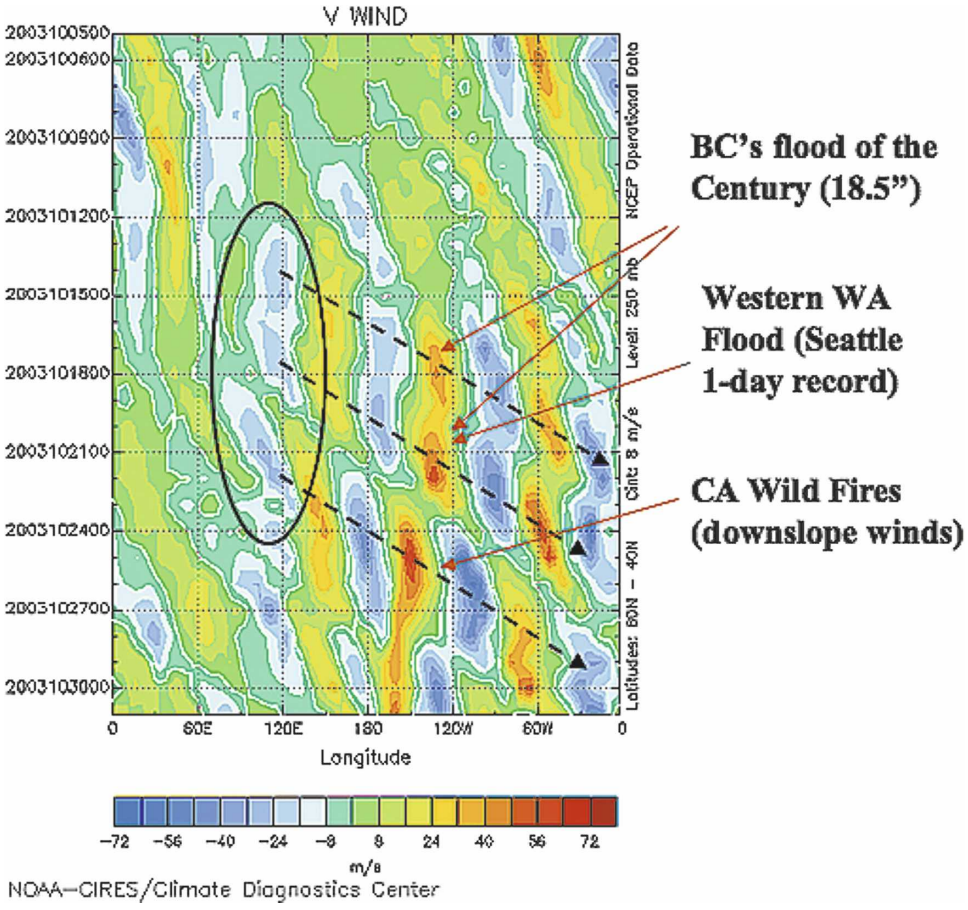

FIG. 1. Time–longitudinal diagram of 250-hPa meridional wind ($m\ s^{-1}$) from 0000 UTC 5 Oct 2003–1200 UTC 31 Oct 2003 (available online at http://www.cdc.noaa.gov). The diagonal dashed lines highlight eastward-moving upper-tropospheric wave packets that originated over eastern Asia (circled area).

westerlies). These wave packets have been extensively studied as packets of Rossby waves (Sardeshmukh and Hoskins 1988; Chang and Yu 1999; Hakim 2003; Chang 2005; and many others). The downstream development of these disturbances has a crucial impact on the weather and climate systems over the North American continent (typically during the fall and winter seasons). Figure 1 is a time–longitudinal diagram of 250-hPa meridional wind ($m\ s^{-1}$) from 0000 UTC 5 October 2003 to 1200 UTC 31 October 2003 (the figure is available online at http://www.cdc.noaa.gov). The dashed diagonal lines highlight eastward-moving upper-tropospheric wave packets that originated over eastern Asia (circled area). These wave trains were responsible for three major weather events that occurred over the west coast of the North American continent during the above-mentioned time: the British Columbia, Canada, flood of the century; the 1-day record flooding in Seattle, Washington; and an outbreak of California wildfires. All three events were poorly forecasted (Parsons et al. 2006).

Several crucial issues to consider related to the forecast of northeastward-propagating Rossby wave trains are the following: What is the exact propagation path for these disturbances traveling along the Rossby wave? Will these disturbances develop into mature extratropical cyclones? How long will these disturbances travel; that is, do they typically dissipate in the middle of the Pacific, or do they cross the entire Pacific basin and eventually make landfall on the west coast of North America? Figures 2a–c are National Oceanic and Atmospheric Administration (NOAA)/Climate Prediction Center (CPC) Morphing Technique (CMORPH) satellite global precipitation estimates for 1 December 2005, 7 January 2006, and 26 Feburary 2006, respectively. We can see that in the Pacific Ocean basin, many of the disturbances/storms are triggered in the tropical western Pacific warm-pool area. These storms then propagate to the northeast, but with different paths. Figure 2a displays a wave train of storms that takes a more zonal path (indicated by the dashed line), directly

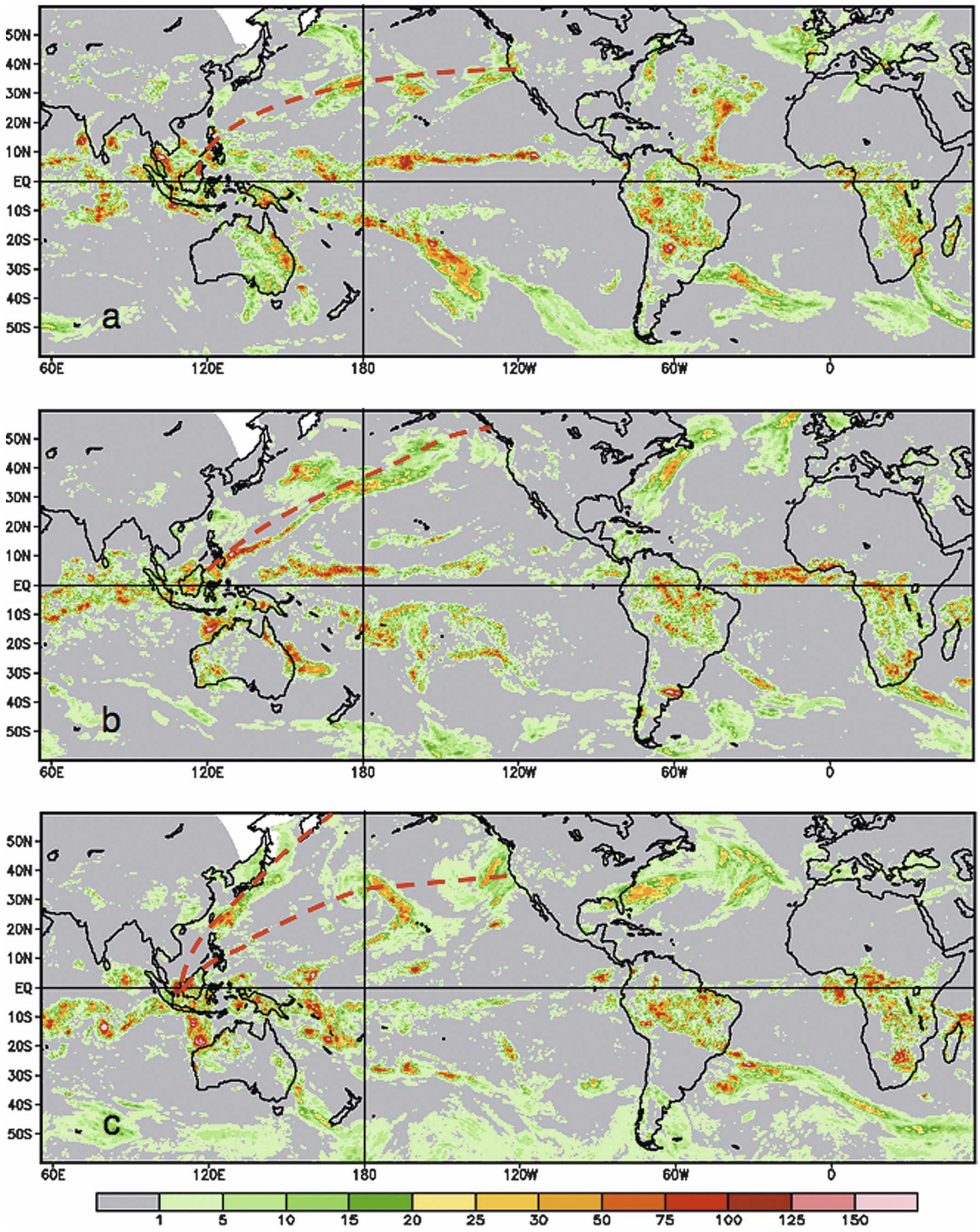

FIG. 2. CMORPH global satellite precipitation estimates (mm day^{-1}) for (a) 1 Dec 2005, (b) 7 Jan 2006, and (c) 26 Feb 2006.

aiming toward the northwest coast of the United States. Figure 2b shows a streamline of storm precipitation that possesses a propagation path with a slightly more meridional component than that in Fig. 2a. The anticipated downstream landfall of this storm system would be on the coastal region of Canada and Alaska. Figure 2c shows two branches of storm propagation: one branch (the lower dashed line) is very similar to the wave train

pattern in Fig. 2a and in a relatively zonal path; the other branch (the upper dashed line) displays a streamline of storm precipitation (similar to that in Fig. 2b), but with a dominant meridional propagation component. The second branch of the storm is most likely to propagate into the North Pacific Ocean and dissipate before reaching the polar region.

From these observational analyses, we can see that tropical weather disturbances are likely the source for tropical and extratropical wave packets. These disturbances typically form as a train of Rossby waves and propagate to the northeast. However, these Rossby wave packets can take different paths, from predominantly zonal to predominantly meridional, as they propagate northeastward. Furthermore, some of these Rossby wave trains may make entire trips across the Pacific Ocean, while others may dissipate in the middle of the Pacific basin. In the following sections, we will explore the possible dynamics that control this variety of Rossby wave propagation patterns.

3. A review of theories about barotropic Rossby wave propagation

The propagation of barotropic Rossby waves has been extensively studied by Hoskins and Karoly (1981), Branstator (1983), Karoly (1983), Hoskins and Ambrizzi (1993), and many others. These classic works are nicely reviewed in James (1994). In this section, we will briefly recapitulate some aspects of these theories.

We begin with the nondivergent barotropic vorticity equation, linearized about a basic state that is a function of latitude only, that is, $\psi(x, y) = \overline{\psi}(y) + \psi'(x, y)$. This linearized vorticity equation is of the form:

$$\frac{\partial}{\partial t}(\nabla^2\psi') + \overline{u}\frac{\partial}{\partial x}(\nabla^2\psi') + \frac{\partial\psi'}{\partial x}\left(\beta - \frac{\partial^2\overline{u}}{\partial y^2}\right) = 0, \tag{3.1}$$

where the overbar denotes a basic state, the prime denotes a departure from the basic state, and $\overline{u} = -\partial\overline{\psi}/\partial y$.

Dropping the prime from the perturbation variable for notational simplicity, we look for a wave solution for (3.1),

$$\psi = Ae^{i\theta}, \tag{3.2}$$

where A is the wave amplitude and $\theta = kx + ly - \omega t$ is the wave phase. The local wavenumbers and frequency can be defined, with respect to this wave phase, as

$$k = \frac{\partial\theta}{\partial x}, \quad l = \frac{\partial\theta}{\partial y}, \quad \text{and} \quad \omega = -\frac{\partial\theta}{\partial t}. \tag{3.3}$$

The above definitions lead to the following wavenumber and frequency relations:

$$\frac{\partial k}{\partial y} = \frac{\partial l}{\partial x}, \quad \frac{\partial k}{\partial t} = -\frac{\partial\omega}{\partial x}, \quad \text{and} \quad \frac{\partial l}{\partial t} = -\frac{\partial\omega}{\partial y}. \tag{3.4}$$

One can derive the dispersion relation for Rossby waves by substituting the wave solution (3.2) into (3.1),

$$\omega = \overline{u}k - \frac{\beta - \partial^2\overline{u}/\partial y^2}{K^2}k, \tag{3.5}$$

where $K^2 = k^2 + l^2$. The two components of the group velocity for steady wave packets are the wavenumber derivatives of the dispersion relation, that is, $\partial\omega/\partial k$ and $\partial\omega/\partial l$, and are, respectively,

$$C_{gx} = \overline{u} + \frac{k^2 - l^2}{K^4}\beta^* \quad \text{and} \quad C_{gy} = \frac{2kl}{K^4}\beta^*, \tag{3.6}$$

where $\beta^* = \beta - \partial^2\overline{u}/\partial y^2$, and subscripts gx and gy denote x and y components of the group velocity. The tendency equation for wave frequency following the wave packet can be derived from relations (3.4) and (3.5),

$$\frac{D_g\omega}{Dt} = \frac{\partial\omega}{\partial t} + C_{gx}\frac{\partial\omega}{\partial x} + C_{gy}\frac{\partial\omega}{\partial y} = 0, \tag{3.7}$$

where $D_g/Dt = \partial/\partial t + C_{gx}\partial/\partial x + C_{gy}\partial/\partial y$ denotes a derivative following a wave packet. Equation (3.7) suggests that the wave packet conserves its frequency during its propagation. This is an important dynamical result. If the Rossby wave excited by a heat source is quasi-stationary at the beginning, the quasi-stationary property will be kept during the course of the energy dispersion. This explains why the 30–60-day low-frequency oscillation forced by tropical deep convections usually has a fixed shape, which presents a quasi-stationary property.

For the quasi-stationary wave (i.e., $\omega \approx 0$), the two components of the group velocity are

$$C_{gx} = \frac{2k^2}{K^2}\overline{u} \quad \text{and} \quad C_{gy} = \frac{2kl}{K^2}\overline{u}, \tag{3.8}$$

where $\overline{u} - K^{-2}(\beta - \partial^2\overline{u}/\partial y^2) = 0$ has been used. Thus, the magnitude of the group velocity is

$$|\mathbf{C}_g| = 2\overline{u}\cos\alpha, \tag{3.9}$$

where $\alpha = \arctan(C_{gy}/C_{gx}) = \arctan(l/k)$. It can be seen from (3.9) that, if the quasi-stationary Rossby wave packet propagates exactly east–west, the magnitude of group velocity $|\mathbf{C}_g|$ is just twice as large as the zonal basic flow $\overline{u}$. When the wave packet approaches the meridional propagation, the group velocity decreases dramatically.

The similar tendency equations describing the evolution of wavenumbers following the wave packet may be expressed as

$$\frac{D_g k}{Dt} = \frac{\partial k}{\partial t} + C_{gx}\frac{\partial k}{\partial x} + C_{gy}\frac{\partial k}{\partial y} = 0 \quad \text{and} \tag{3.10}$$

$$\frac{D_g l}{Dt} = \frac{\partial l}{\partial t} + C_{gx}\frac{\partial l}{\partial x} + C_{gy}\frac{\partial l}{\partial y} = \frac{k}{K^2}\frac{\partial \beta^*}{\partial y} - k\frac{\partial \overline{u}}{\partial y}. \tag{3.11}$$

As is apparent from these relations, the wave packet conserves its zonal wavenumber during its propagation because the dispersion relation is independent of x. On the other hand, because the basic flow $\overline{u}$ varies in the y direction, the meridional wavenumber is *not* conserved.

Because of the quasi-stationarity of the waves representing the low-frequency variations, the magnitude of their meridional wavenumber l can be estimated by substituting $\omega \approx 0$ into Eq. (3.5), namely,

$$l = \pm\left[\left(\beta - \frac{\partial^2 \overline{u}}{\partial y^2}\right) \Big/ \overline{u} - k^2\right]^{1/2}. \tag{3.12}$$

If the solution of l to (3.12) is imaginary, the meridional propagation is not possible. Even for a purely zonal disturbance, l only equals 0, rather than an imaginary value. Meanwhile, it should be noted that β is always positive and its magnitude is generally larger than $\partial^2\overline{u}/\partial y^2$ in the Northern Hemisphere. Therefore, there is no meridional propagation of Rossby waves when $\overline{u} < 0$. This explains why those barotropic Rossby waves that are driven by heating near the equator, where the easterly winds prevail, are in the mid- to upper troposphere.

Defining $K_s = [(\beta - \partial^2\overline{u}/\partial y^2)/\overline{u}]^{1/2}$, Eq. (3.12) can be rewritten as

$$l = \pm\sqrt{K_s^2 - k^2}. \tag{3.13}$$

We now consider a simple analytical case. Assume that the zonal basic flow linearly varies with y, namely, $\overline{u} = u_0 y$, where u_0 is a positive constant. If $k < K_s$, the positive and negative roots of (3.13) correspond to the propagations of Rossby waves into the Northern and the Southern Hemispheres, respectively. When the wave propagates toward the lower latitudes, K_s will increase because $\overline{u}$ decreases. At some latitude where the westerly wind switches to the easterly wind, K_s becomes extremely large so that l becomes increasingly large according to Eq. (3.13). This latitude where $k\overline{u} = \omega(\omega \approx 0$ in the present case) is the "critical latitude" (Dickinson 1968; Adams 1986). The meridional scale of the Rossby waves becomes extremely small (for extremely large l). Thus, the equatorward-propagating ray will be more meridionally directed. It can be inferred from Eq. (3.9) that the group velocity $\mathbf{C}_g$ becomes very small. Therefore, as such a latitude is approached, the wave packet propagates extremely slowly in a nearly meridional direction. Indeed, the wave packet will, according to this linear, inviscid theory, reach the critical latitude only in infinite time, effectively being absorbed. Thus, the critical latitude acts as a "black hole" on the Rossby wave. Nonlinear effects, not discussed here, can cause partial reflection (Tung 1979; Haberman 1972, 1976).

For the poleward-propagating ray, the wave packet moves into an environment where K_s become smaller because $\overline{u}$ increases. As K_s becomes small, the wave packet adjusts itself by acquiring a small l, that is, by extending more in the meridional direction. The ray will take a more zonal direction. Eventually, at a latitude where $K_s = k$, l becomes 0. As such a latitude is approached, the meridional wavenumber continues to decrease and then gradually becomes negative according to (3.13). At this latitude, the ray is reflected back into the lower latitudes. This depicts the great circle track theory regarding the propagation of the two-dimensional Rossby wave packet (Longuet-Higgins 1964; Hoskins and Karoly 1981). Note that this great circle wave track theory permits the propagation of Rossby waves through the equatorial easterly for $C < 0$, where C is a phase velocity. However, for $C > 0$, their meridional propagation can only occur in the westerly region.

4. The propagation of barotropic Rossby waves with divergence

In this section, we extend the classic theories (from the previous section) on barotropic Rossby wave propagation, with a consideration of divergence effect. For a barotropic flow on the β plane, the vorticity equation takes the form

$$\frac{\partial \zeta}{\partial t} + u\frac{\partial \zeta}{\partial x} + v\frac{\partial \zeta}{\partial y} + \beta v = -(f + \zeta)D, \tag{4.1}$$

where ζ is the vertical component of relative vorticity and D is the horizontal divergence.

Partition wind components, vertical vorticity, and horizontal divergence into basic states and perturbations

$$\begin{aligned} u(x, y) &= \overline{u}(y) + u'(x, y), \\ v(x, y) &= v'(x, y), \\ \zeta &= \overline{\zeta} + \zeta', \quad \text{and} \\ D &= \overline{D} + D', \end{aligned} \tag{4.2}$$

where the overbar, again, denotes a basic state and the prime represents departure from the basic state. On

substituting (4.2) into (4.1), one obtains the linearized perturbation vorticity equation

$$\frac{\partial \zeta'}{\partial t} + \overline{u}\frac{\partial \zeta'}{\partial x} + \left(\beta - \frac{\partial^2 \overline{u}}{\partial y^2}\right)v' = -(f + \overline{\zeta})D'. \quad (4.3)$$

The perturbation winds can be divided into rotational and divergent parts, that is, $v' = v'_\psi + v'_\chi$, $v'_\psi = k \times \nabla\psi$, and $v'_\chi = \nabla\chi$, where ψ and χ are perturbation streamfunction and velocity potential, respectively. Under this partition, Eq. (4.3) becomes

$$\frac{\partial \zeta'}{\partial t} + \overline{u}\frac{\partial \zeta'}{\partial x} + \left(\beta - \frac{\partial^2 \overline{u}}{\partial y^2}\right)v'_\psi = -(f + \overline{\zeta})D' - \left(\beta - \frac{\partial^2 \overline{u}}{\partial y^2}\right)v'_\chi. \quad (4.4)$$

Equation (4.4) states that the local change of perturbation vorticity is determined by the basic-state flow, basic-state vorticity, β factor, rotational wind and divergence, as well as divergent wind.

With the assumption that the basic state varies very slowly, we look for a solution to (4.4) in the WKB forms

$$\psi = A(X, Y, T)e^{i[\varepsilon^{-1}(kX + lY - \omega T)]}, \quad (4.5)$$

$$\chi = \lambda A(X, Y, T)e^{i[\varepsilon^{-1}(kX + lY - \omega T) - \delta]}, \quad (4.6)$$

where $(X, Y, T) = \varepsilon(x, y, t)$ represents slow time and spatial scales, in which case $|\varepsilon| < 1$, δ is the phase difference between velocity potential and streamfunction, and λ is the ratio of the amplitude of velocity potential to that of streamfunction. Using (4.5) and (4.6), it is easily verified that

$$v'_\psi = \frac{\partial \psi}{\partial X}, \quad v'_\chi = \frac{\partial \chi}{\partial Y}, \quad \zeta' = \nabla^2\psi, \quad \text{and} \quad D' = \nabla^2\chi, \quad (4.7)$$

where $\nabla^2 = (\partial^2/\partial X^2 + \partial^2/\partial Y^2)$ is a Laplacian operator. Because this study is to examine the propagation of Rossby waves rather than wave instability, the frequency ω is supposed to be real and positive.

Substituting (4.5), (4.6), and (4.7) into (4.4), the zeroth-order equation (when k and l are large) is

$$i(\omega - \overline{u}k)(k^2 + l^2) + ik\left(\beta - \frac{\partial^2 \overline{u}}{\partial Y^2}\right) = \lambda\left(f - \frac{\partial \overline{u}}{\partial Y}\right)(k^2 + l^2)(\cos\delta - i\sin\delta) - \lambda l\left(\beta - \frac{\partial^2 \overline{u}}{\partial Y^2}\right)(i\cos\delta + \sin\delta). \quad (4.8)$$

The dispersion relation and the phase difference equation for the low-frequency Rossby wave can be obtained by separating real and imaginary parts in (4.8). In doing so, one can obtain

$$\omega = \overline{u}k - \frac{(\beta - \partial^2 \overline{u}/\partial Y^2)}{k^2 + l^2}\left(k + \frac{\lambda l}{\cos\delta}\right), \quad (4.9)$$

$$\cot\delta = \frac{\beta - \partial^2 \overline{u}/\partial Y^2}{f - \partial \overline{u}/\partial Y}\frac{l}{k^2 + l^2}. \quad (4.10)$$

It can be seen that the frequency ω closely depends on the zonal basic flow, β factor, meridional gradient of the basic absolute vorticity, phase difference, wavenumbers, and divergent wind. The phase difference δ is a function of local wavenumbers, basic absolute vorticity, and meridional gradient of basic absolute vorticity. In the absence of divergent wind (i.e., $\lambda = 0$), Eq. (4.9) reduces to the classic dispersion relation for two-dimensional Rossby waves [Eq. (3.5)]. Using a quasi-stationary approximation ($\omega \approx 0$) in (3.5) and substituting the result into (4.10), one can conclude that for nondivergent approximation $\lambda = 0$, $\cot\delta$ is extremely large, so that $\delta \to 0$. This means that if there is no divergence involved in the barotropic vorticity equation, there will not be an issue of phase difference, which is certainly the idealized case for the classic Rossby wave propagation theory (Hoskins and Karoly 1981; Branstator 1983; Karoly 1983; Hoskins and Ambrizzi 1993).

The term $-\lambda l(\beta - \partial^2 \overline{u}/\partial Y^2)/[(k^2 + l^2)\cos\delta]$ in (4.9) represents a contribution of divergence to the wave frequency. If both l and $\beta - \partial^2 \overline{u}/\partial Y^2$ are positive for δ located in the first quadrant, the divergent wind will increase the periods of Rossby waves. The stronger the divergence, the longer the wave period becomes. When the values of $f - \partial \overline{u}/\partial Y$, $\beta - \partial^2 \overline{u}/\partial Y^2$, and l are positive, it follows from (4.10) that the range of phase difference varies from 0 to $\pi/2$, namely, $0 < \delta < \pi/2$, which can be interpreted physically that at upper levels, the divergence center lies somewhere in front of the trough line and the convergence center lies somewhere behind the trough line.

The components of the group velocity can be easily derived from (4.9),

$$C_{gx} = \frac{\partial \omega}{\partial k} = \overline{u} + \frac{\beta - \partial^2 \overline{u}/\partial Y^2}{(k^2 + l^2)^2}(k^2 - l^2 + 2\lambda kl\cos\delta), \quad (4.11)$$

$$C_{gy} = \frac{\partial \omega}{\partial l} = \frac{\beta - \partial^2 \overline{u}/\partial Y^2}{(k^2 + l^2)^2}[2kl + \lambda\cos\delta(l^2 - k^2)], \quad (4.12)$$

which differ from those given by Hoskins and Karoly [1981, their Eq. (3.6)] because of the additional terms related to the divergence. But again, when the divergent flow is neglected (by taking $\lambda = 0$), (4.11) and (4.12) reduce to their (3.6). The term $2\lambda kl \cos\delta(\beta - \partial^2\overline{u}/\partial Y^2)/(k^2 + l^2)^2$ in (4.11) indicates that the divergent wind would increase the zonal group velocity and accelerate the zonal propagation of Rossby waves if $\delta \in (0, \pi/2)$, $k > 0$, $l > 0$, and $\beta - \partial^2\overline{u}/\partial Y^2 > 0$. The term $\lambda(l^2 - k^2)\cos\delta(\beta - \partial^2\overline{u}/\partial Y^2)/(k^2 + l^2)^2$ in (4.12) implies that for $\beta - \partial^2\overline{u}/\partial Y^2 > 0$, $l > k$, and $\delta \in (0, \pi/2)$, the divergent wind will increase the meridional group velocity and is favorable for the meridional propagation of Rossby waves. However, when Rossby wave energy is dispersed to the midlatitudes, l is usually smaller than k and the divergent wind tends to retard the meridional propagation of Rossby waves.

Denoting $m = [l^2 + (f - \partial\overline{u}/\partial Y)^2(k^2 + l^2)^2/(\beta - \partial^2\overline{u}/\partial Y^2)^2]^{1/2}$, the two components of the group velocity can be expressed as

$$C_{gx} = \frac{\partial\omega}{\partial k} = \overline{u} + \frac{(\beta - \partial^2\overline{u}/\partial Y^2)}{(k^2 + l^2)^2}\left(k^2 - l^2 + \frac{2\lambda l^2 k}{m}\right), \tag{4.13}$$

$$C_{gy} = \frac{\partial\omega}{\partial l} = \frac{(\beta - \partial^2\overline{u}/\partial Y^2)}{(k^2 + l^2)^2}\left[2kl + \frac{\lambda l(l^2 - k^2)}{m}\right]. \tag{4.14}$$

Following Yang and Hoskins (1996) and Karoly (1983), it is clear from (4.13) and (4.14) that when the Rossby wave meets the reflection latitude, that is, $l \to 0$, C_{gy} is close to zero. At such a line, the Rossby wave zonally propagates at the group velocity of $C_{gx} = \overline{u} + (\beta - \partial^2\overline{u}/\partial Y^2)/k^2$ and the Rossby wave turns, moving southward in the meridional direction. At the critical latitude, $l \to \infty$, C_{gy} also tends to be zero, which indicates that Rossby wave energy is trapped in the meridional direction, and Rossby waves propagate with the basic flow speed ($C_{gx} = \overline{u}$). At the reflection and critical latitudes, the divergent wind does not influence on the group velocity.

5. Ray-tracing diagnostics of Rossby wave propagation with a realistic zonal flow

The ray shows the path along which the Rossby wave energy is dispersed. Given the analytic expressions for the 2D group velocity in (4.11)–(4.12), or alternatively in (4.13)–(4.14), the ray equations can be written

$$\frac{dx}{dt} = C_{gx}, \quad \frac{dy}{dt} = C_{gy}. \tag{5.1}$$

When this pair of equations is integrated, a parameterized curve $[x(t), y(t)]$ is obtained. This curve is the ray of Rossby wave propagation.

Because (4.9) and (4.10) are independent of x and t, ω and k are constant along a ray path, as described in (3.7) and (3.10). However, l varies along the ray path because (4.9) and (4.10) do depend on y. The variation of l is easily obtained by requiring that the local relations (4.9) and (4.10) are satisfied. The ray path is computed by integrating the differential Eqs. (5.1) for a given initial position (x_0, y_0), λ, ω, and k. To simplify the analysis of the influence of divergent wind on the Rossby wave propagation, we only consider Rossby waves that propagate out of the tropics. In this case, as discussed in the previous sections, the meridional wavenumber is positive so that the wave propagates poleward.

The basic flow used in this computation is a climatological 300-hPa zonal-mean flow for DJF based on NCEP–NCAR reanalysis monthly data for the period of 1997–98 (Fig. 3). This basic-state zonal flow displays weak easterlies in the vicinity of the equator, strong westerlies in the midlatitudes of both hemispheres, and weak westerlies near the poles. The initial position is chosen as 15°N, 115°E, where the west Pacific warm pool is located. Low-frequency Rossby waves are most likely generated in response to the deep tropical convection in this region. For all cases presented below, the rays are truncated just prior to reaching turning points. These are the locations where Rossby wave packets are trapped and reflect equatorward.

a. Ray tracing for planetary- and synoptic-scale Rossby waves in the Pacific Ocean basin

Two sets of waves are selected to represent planetary- and synoptic-scale wave motions in the atmosphere. The planetary waves are represented by zonal wavenumbers 3 and 4, equivalent to zonal wavelengths of about 9000–12 500 km. The synoptic waves possess zonal wavenumbers 5 and 6, and they correspond to zonal wavelengths of about 6000–7500 km.

To evaluate the effects of divergence on the Rossby wave ray tracing, we also select a set of λ parameters, denoting different strengths of divergent winds relative to their rotational counterparts. In the midlatitude, the observations typically show that vorticity is about 10 times as large as divergence. Therefore, in the following experiments, the λ parameters are set to 0.1, 0.05, and 0 to mimic a relatively strong divergence, a medium-strength divergence, and a pure nondivergent flow, respectively.

Figure 4a shows the rays of low-frequency Rossby waves with divergent wind for the periods of 30 days.

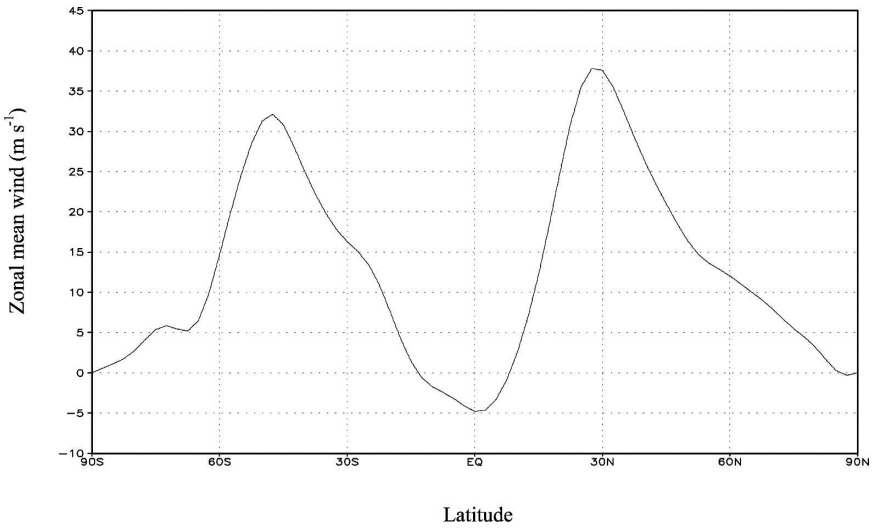

FIG. 3. Zonal-mean zonal flow at 300 hPa averaged over DJF 1997–98.

We choose $\lambda = 0.1$ for this case, which means that the amplitude of vorticity is 10 times as large as that of divergence. For the period of 30 days, all low-frequency Rossby waves propagate toward the northeast. The paths of different waves are segments of different great arcs, similar to that in Hoskins and Karoly (1981). These waves all have a tendency to propagate toward the northwestern coast of the United States. In particular, the high-wavenumber (synoptic scale) waves are more "energetic" than the low-wavenumber (planetary scale) waves, in the sense that they propagate farther.

However, for $\lambda = 0.05$, the rays shown in Fig. 4b have some significantly different features from those in Fig. 4a. All of those waves reach higher latitudes, except for the wave with zonal wavenumber 6, which is trapped in the middle of the Pacific. Although all these rays are segments of different great arcs, these waves possess stronger meridional components than those in Fig. 4a, and target the coasts of Canada and Alaska. For example, the Rossby wave with $k = 5$ propagates faster than other waves after 30 days, reaching 58°N. The same wave in Fig. 4a, with stronger divergent winds, reaches only 50°N.

In the absence of divergent wind (Fig. 4c) for $\lambda = 0$, although Rossby waves also propagate toward the northeast, the ray paths show an even stronger meridional component. For example, for $k = 3$ and 4, nondivergent Rossby waves propagate farther to the north and the ray paths are more meridionally oriented than the divergent Rossby waves. The ray paths for $k = 5$ and 6 are very short, and they are trapped around the ET region. This implies (in reference to Fig. 4a) that without strong divergent effects, the synoptic-scale waves do not have enough strength to travel very far from their source region. The planetary-scale waves, on the other hand, can easily pass the ET region, regardless of the divergent effects.

The effect of divergence on the long-period Rossby wave is shown in Fig. 5 (with $\lambda = 0.1$). For the 60-day period, the Rossby waves with zonal wavenumbers 3, 4, and 5 display approximately the same propagation paths (Fig. 4a) as those for the 30-day period. The only exception is for the wave with zonal wavenumber 6, which was trapped prematurely in the middle of the Pacific and stopped at 37°N. This implies that the divergence has a stronger effect on the high-wavenumber waves for longer period. The waves propagating toward the high latitudes and farther east reach 50°, 45°, and 40°N, for $k = 5$, 4, and 3, respectively.

In comparing all three cases, one can see that divergence tends to enforce the zonal component of group velocity and reduce the meridional group velocity. For synoptic-scale waves, without divergence, they tend to be trapped close to their source region. Divergence appeared to provide some additional energy for these high-wavenumber waves to pass over the low- to middle-latitude "barrier," where they were often trapped. For example, when $\lambda = 0.05$ (Fig. 4b), wavenumber 5 is "released" from its trap (cf. with Fig. 4c). By further increasing the λ value, wavenumber 6 may also be released (Fig. 4a). All these results are consistent with (4.11) and (4.12). According to (4.11) and (4.12), λ always increases C_{gx}, and tends to decrease C_{gy} when $k > l$. Without a divergence effect, for relatively high-zonal-wavenumber waves, both C_{gx} and C_{gy} tend to be smaller [due to a larger denominator in (4.11) and (4.12)] than low-zonal-wavenumber waves. When divergence is added, the increased value in C_{gx} and C_{gy}

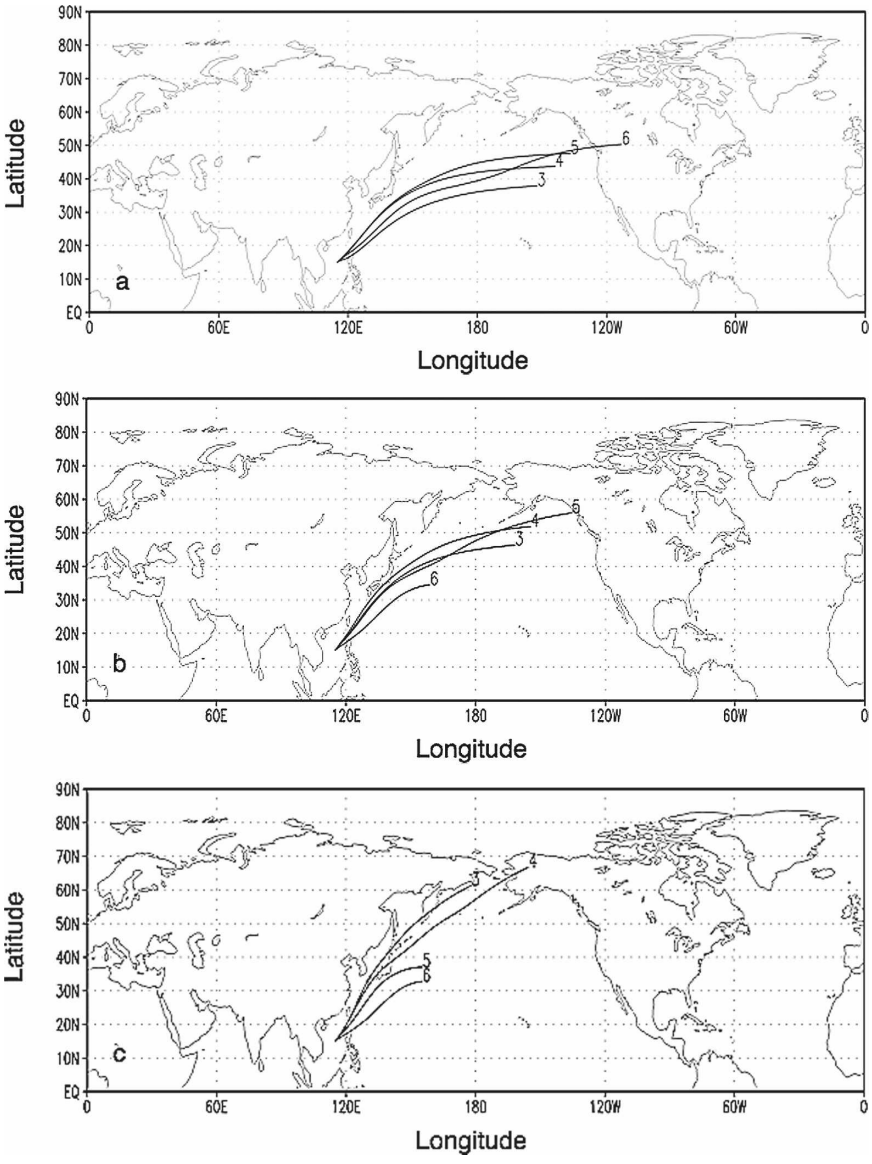

FIG. 4. The ray paths of Rossby waves for a period of 30 days, with (a) a strong divergent wind ($\lambda = 0.1$), (b) a medium-strength divergent wind ($\lambda = 0.05$), and (c) no divergent wind ($\lambda = 0.0$). The source is at 15°N, 115°E. The waves travel through a basic flow of the DJF zonal flow. The numbers denote zonal wavenumbers.

may overcome the decreasing effect resulting from high zonal wavenumbers.

While the present theory for divergent Rossby wave propagation is self-consistent as analyzed above, how does it compare to observations? The observational analyses in section 2 identified three different Rossby wave tracks in the Pacific Ocean basin. Our calculations for three different divergent forcing scenarios result in Rossby wave ray paths that explain those observations quite reasonably. Other observational evidence is also in favor of the present theoretical results. For example, Kiladis and Weickmann (1992) investigated the response of waves to tropical convection during a Northern Hemisphere winter by analyzing outgoing longwave radiation (OLR) and NCEP's global analyses. They found that for the 30–70-day oscillations, the upper-level circulation signals are zonally elongated, with dominant low zonal wavenumbers (0–2). For the 14–30-day oscillation, smaller-scale signals of wavenumbers 5 and 6 are important. By comparing Figs. 4a and 5, we do see the zonally elongated trajectory of Rossby waves in this divergent theory. In addition, relatively

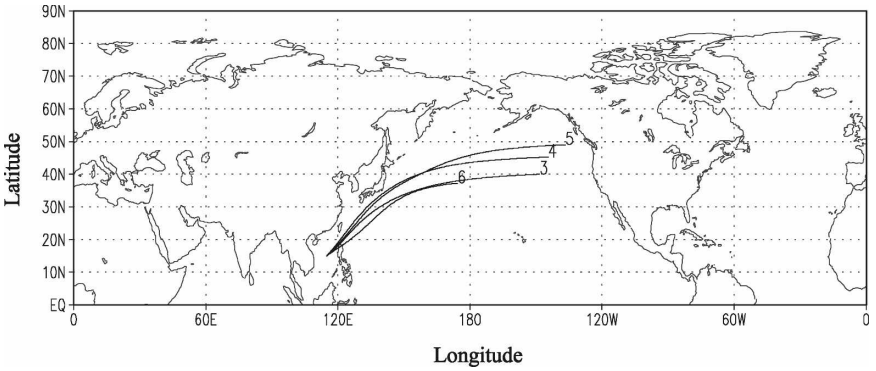

FIG. 5. Same as in Fig. 4, except for a period of 60 days, and with a strong divergent wind ($\lambda = 0.1$).

speaking, the 60-day period (Fig. 5) gave more weight to the lower-wavenumber waves (3–4) propagating downstream, while for the 30-day period (Fig. 4a) the higher-wavenumber waves (5–6) had a strong presence in the propagating wave packet. These results are all in agreement with the observational study by Kiladis and Weickmann (1992), at least in a qualitative sense.

In contrast, the results for the nondivergent theory (Fig. 4c) do not agree with the cited observations. This indicates that the present divergent theory improves the classic nondivergent theory, and qualitatively explains the available observations.

b. Upper-level vorticity and divergence coupling

One of the important issues when divergence is included in the barotropic vorticity system is how vorticity and divergence are coupled. The classic baroclinic model indicates that the surface cyclonic center is typically associated with flow convergence, but the upper-level convergence/divergence flows are not collocated with trough/ridge centers. The upper-level trough is typically tilted to the west of a surface low center. In other words, there exists a phase difference between convergence/divergence and the trough/ridge region at upper levels. As analyzed in the previous section, the present theory predicts a phase between the divergence and vorticity in a range of $(0, \pi/2)$. It is interesting to note that although the present divergent barotropic theory cannot capture the vertical structure of baroclinic waves, it does reasonably describe the horizontal structure of these waves at free atmosphere (no surface friction or an Ekman effect). In this section, we examine how this phase is evolving and developing along the ray path. Given constant zonal wavenumbers and the structure of basic zonal flow, the phase can be calculated using (4.10). Because the meridional wavenumber l changes with time, the calculated phase is a function of time as well.

Figure 6 summarizes the phase difference in terms of the zonal wavenumber k and as a function of time, restricted to $l > 0$ (poleward propagation). At an initial stage, the phase differences decrease. After 1 or 2 days, the phase differences begin to increase and approach $\pi/2$. The synoptic-scale waves (zonal wavenumbers 5 and 6) reach a $\pi/2$ phase locking in about 2 days. It takes 3 days for wavenumber 4 to have the phase difference saturated at the value of $\pi/2$. The planetary-scale wave (wavenumber 3) evolves very slowly (5 days) toward $\pi/2$ phase locking. These results all seem physically reasonable. First, they suggest that the vorticity center lags behind the divergence center by $\pi/2$ phase at upper levels. Second, for synoptic-scale waves, it is faster for divergence and vorticity to be locked in phase; for planetary waves, this phase locking takes a much longer time to develop. Physically, this may be interpreted as the synoptic-scale waves needing to respond to convective heating relatively quickly, on account of their shorter life span of a few days. The planetary-scale waves, on the other hand, respond to convective heating relatively slowly because of their longer life span.

While these results are consistent with the classic baroclinic theory, they are also in agreement with the observational study by Kiladis and Weickmann (1992). The cited study found that for three scale oscillations: 30–70, 14–30, and 6–14-day oscillations, OLR anomalies (a divergence/convergence center) peak prior to the upper-level circulation anomalies (a vorticity center) in all three time scales.

6. Conclusions

In this study, the effect of divergence on Rossby wave propagation is examined. A two-dimensional WKB analysis and the ray-tracing technique are used. This problem is treated within a linear, divergent barotropic

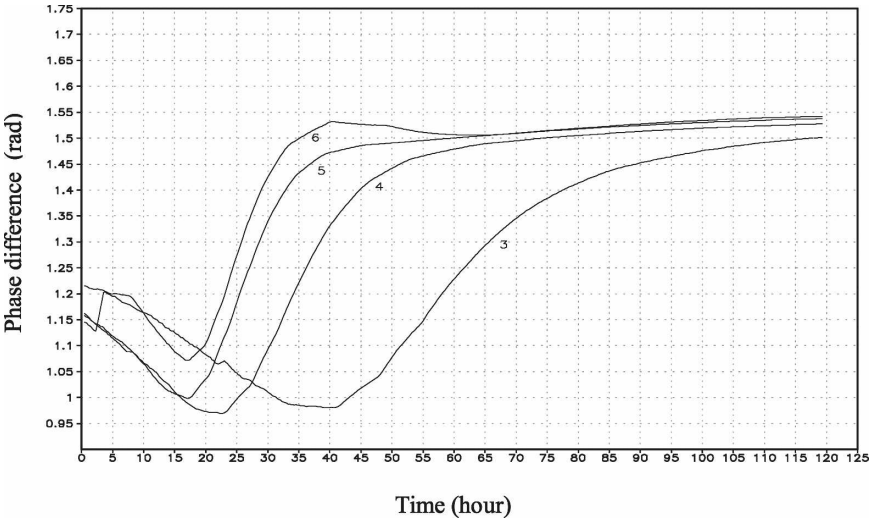

FIG. 6. Temporal evolution of phase differences between streamfunction and velocity potential for a 30-day period in the case with divergence. The numbers denote zonal wavenumbers.

dynamic framework. The results generalize and extend the classic theories for Rossby wave propagation.

The WKB analysis shows that Rossby wave frequency is determined by a combination of basic-state flow, meridional gradient of basic absolute vorticity, local wavenumbers, and two parameters coupling vorticity and divergence. The first parameter measures the degree of divergent flow relative to rotational flow. The second parameter is the phase difference between vorticity and divergence. An analytic expression for the phase difference is also derived from the WKB analysis. This parameter is dependent on local wavenumbers, absolute vorticity, and its meridional gradient. With these analytic results, 2D group velocity can be derived, and thus the ray equations can be defined and integrated.

The contribution of divergent wind is to increase the period of the Rossby wave (for $l > 0$, i.e., wave propagation northward in the Northern Hemisphere). Ray-tracing analysis has provided further insights into the effect of divergence on the group velocity and the path of energy propagation. Divergent wind enlarges the zonal group velocity component and accelerates the zonal propagation of Rossby waves if the phase difference δ falls into $(0, \pi/2)$. For $l < k$, divergent wind plays a role in reducing the meridional component of group velocity and slows meridional energy propagation. Integration of the ray equations with a realistic DJF basic flow shows that the path of propagation of low-frequency Rossby waves with divergent wind is a smooth arc. For planetary-scale waves, the weaker the divergent wind, the stronger of the meridional propagation and the higher the latitudes that the waves reach; for synoptic-scale waves, the stronger the divergent wind, the larger the potential for these waves to propagate downstream. The phase difference between vorticity and divergence is close to $\pi/2$ at an upper level of atmosphere when Rossby waves propagate into middle latitudes, which is consistent with the realistic situation.

Finally, the theoretical results obtained in this investigation may have some practical significance for the improvement of forecasting the high-impact weather systems that pose a threat to the west coast of North America (discussed in section 2). In particular, the diagnosis of divergent winds in the tropical and extratropical storms in the Pacific basin may provide forecast guidance for the strength and tracks of these storms.

Acknowledgments. The authors thank Dr. Linkun Ren for providing the computations of Rossby wave ray tracing and Ann Reiser for her technical editing of this paper. We would also like to thank Professor K. K. Tung for his excellent editorship, and two anonymous reviewers for their constructive comments and suggestions. This work is supported by the National Oceanic and Atmospheric Administration and by the National Science Foundation through Grant OCE 0451951.

REFERENCES

Adam, J. A., 1986: Critical layer singularities and complex eigenvalues in some differential equations of mathematical physics. *Phys. Rep.,* **142,** 263–356.

Bennett, J. R., and J. A. Young, 1971: The influence of latitudinal wind shear upon large-scale wave propagation into the tropics. *Mon. Wea. Rev.,* **99,** 202–214.

Boyd, J. P., 1978: The effects of latitudinal shear on equatorial waves. Part I: Theory and methods. *J. Atmos. Sci.,* **35,** 2236–2258.

——, 1982: The influence of meridional shear on planetary waves. Part 2: Critical latitudes. *J. Atmos. Sci.,* **39,** 770–790.

Branstator, G., 1983: Horizontal energy propagation in a barotropic atmosphere with meridional and zonal structure. *J. Atmos. Sci.,* **40,** 1689–1708.

Chang, E. K. M., 2005: The impact of wave packets propagating across Asia on Pacific cyclone development. *Mon. Wea. Rev.,* **133,** 1998–2015.

——, and D. B. Yu, 1999: Characteristics of wave packets in the upper troposphere. Part I: Northern Hemisphere winter. *J. Atmos. Sci.,* **56,** 1708–1728.

Cressman, G. P., 1958: Barotropic divergence and very long atmospheric waves. *Mon. Wea. Rev.,* **86,** 293–297.

Dickinson, R. E., 1968: Planetary Rossby waves propagating vertically through weak westerly wind wave guides. *J. Atmos. Sci.,* **25,** 984–1002.

Ferranti, L., T. N. Palmer, F. Molteni, and E. Klinker, 1990: Tropical–extratropical interaction associated with the 30–60 day oscillation and its impact on medium and extended range prediction. *J. Atmos. Sci.,* **47,** 2177–2199.

Gao, S., S. Tao, and Y. Ding, 1990: The generalized E-P flux of wave-mean flow interactions. *Sci. China,* **33B,** 704–715.

Haberman, R., 1972: Critical layers in partial flows. *Stud. Appl. Math.,* **51,** 139–161.

——, 1976: Non-linear perturbations of the Orr-Sommerfeld equation—Asymptotic expansion of the logarithmic phase across the critical layer. *SIAM J. Math. Anal.,* **7,** 70–81.

Hakim, G. J., 2003: Developing wave packets in the North Pacific storm track. *Mon. Wea. Rev.,* **131,** 2824–2837.

Hoskins, B. J., and D. J. Karoly, 1981: The steady linear response of a spherical atmosphere to thermal and orographic forcing. *J. Atmos. Sci.,* **38,** 1179–1196.

——, and T. Ambrizzi, 1993: Rossby wave propagation on a realistic longitudinally varying flow. *J. Atmos. Sci.,* **50,** 1661–1671.

——, and K. I. Hodges, 2002: New perspectives on the Northern Hemisphere winter storm tracks. *J. Atmos. Sci.,* **59,** 1041–1061.

James, I. N., 1994: *Introduction to Circulating Atmospheres*. Cambridge University Press, 422 pp.

Karoly, D. J., 1983: Rossby wave propagation in a barotropic atmosphere. *Dyn. Atmos. Oceans,* **7,** 111–125.

Kiladis, G. N., and K. M. Weickmann, 1992: Circulation anomalies associated with tropical convection during northern winter. *Mon. Wea. Rev.,* **120,** 1900–1923.

——, and ——, 1997: Horizontal structure and seasonality of large-scale circulations associated with submonthly tropical convection. *Mon. Wea. Rev.,* **125,** 1997–2013.

Klein, P. M., P. A. Harr, and R. Elsberry, 2002: Extratropical transition of western North Pacific tropical cyclones: Midlatitude and tropical cyclone contributions to reintensification. *Mon. Wea. Rev.,* **130,** 2240–2259.

Kundu, P. K., 1990: *Fluid Mechanics*. Academic Press, 638 pp.

Lindzen, R. S., and J. R. Holton, 1968: A theory of the quasi-biennial oscillation. *J. Atmos. Sci.,* **25,** 1095–1107.

Longuet-Higgins, M. S., 1964: Planetary waves on a rotating sphere. *Proc. Roy. Soc. London,* **279A,** 446–473.

Madden, R. A., and P. R. Julian, 1971: Detection of a 40–50 day oscillation in the zonal wind in tropical Pacific. *J. Atmos. Sci.,* **28,** 702–708.

——, and ——, 1972: Description of global-scale circulation cells in the tropics with a 40–50 day period. *J. Atmos. Sci.,* **29,** 1109–1123.

Matsuno, T., 1971: A dynamic model of stratospheric sudden warming. *J. Atmos. Sci.,* **28,** 1479–1494.

Parsons, D., I. Szunyogh, and P. Harr, 2006: Scientific program overview: THORPEX Pacific-Asian Regional Campaign (T-PARC). UCAR, 18 pp. [Available online at http://www.ucar.edu/na-thorpex/tparc.]

Rossby, C.-G., 1939: Relation between variations and the intensity of the zonal circulation of the atmosphere and the displacements of the semi-permanent centers of action. *J. Mar. Res.,* **2,** 38–55.

——, 1945: On the propagation of frequencies and energy in certain types of oceanic and atmospheric waves. *J. Meteor.,* **2,** 187–204.

Sardeshmukh, P. D., and B. J. Hoskins, 1988: The generation of global rotational flow by steady idealized tropical divergence. *J. Atmos. Sci.,* **45,** 1228–1251.

Tung, K. K., 1979: A theory of stationary long waves. Part III: Quasi-normal modes in a singular waveguide. *Mon. Wea. Rev.,* **107,** 751–774.

Wallace, J. M., and D. S. Gutzler, 1981: Teleconnections in the geopotential height field during the Northern Hemisphere winter. *Mon. Wea. Rev.,* **109,** 784–812.

——, and M. L. Blackmon, 1983: Observations of low-frequency atmospheric variability. *Large-scale Dynamic Processes in the Atmosphere,* B. Hoskins and R. Pearce, Eds., Academic Press, 55–94.

Yang, G.-Y., and B. J. Hoskins, 1996: Propagation of Rossby waves of nonzero frequency. *J. Atmos. Sci.,* **53,** 2365–2378.

Yeh, T., 1949: On energy dispersion in the atmosphere. *J. Meteor.,* **6,** 1–16.